Iterative Learning Control of Supersaturation in Batch Cooling Crystallization

Marco Forgione, Ali Mesbah, Xavier Bombois and Paul M.J. Van den Hof

Abstract— An Iterative Learning Control (ILC) algorithm for supersaturation control in batch cooling crystallization is presented in this paper. The ILC controller is combined with a PI controller in order to reject the disturbances present in the thermal dynamics as much as possible. Convergence and robustness properties of the proposed ILC+PI control scheme are investigated. The simulation studies reveal that the controller is well capable of tracking a predetermined supersaturation trajectory in the presence of model imperfections, measurement noise and actuation deficiencies.

I. INTRODUCTION

Crystallization can be defined as a phase change in which a solid crystalline product is obtained from a solution [1]. The crystalline material is formed from the fluid phase, making crystallization a core separation and purification technology in the pharmaceutical, food and fine chemical industries [2]. Crystallization processes are often operated in batch mode. Batch processes are particularly convenient when production volumes are low, when isolation is necessary, and when frequent changeovers are required. In this paper we restrict our attention to batch cooling crystallization, which is the most widely applied crystallization method.

The current practice in operation of industrial batch cooling crystallization processes is to control the temperature inside the crystallizer to follow a desired profile during the batch [3]. The process variable that can be manipulated to influence the temperature inside the crystallizer is the temperature of a jacket on the crystallizer. Since accurate on-line temperature measurements can readily be obtained, the temperature is usually controlled in a closed-loop setting. In this configuration, the desired crystallizer temperature is given as reference trajectory of a feedback loop. This strategy is known as T-control in literature [3]. Due to disturbances affecting the jacket temperature and model uncertainties, such a closed-loop configuration is essential in order to follow the temperature profile accurately.

However, even when temperature is accurately controlled, the final product of a batch might not show the expected characteristics. Furthermore, the result might not be reproducible from one batch to the other. Even though temperature is an important process variable, it is not the one most closely related to the crystallization dynamics. The variable having the most direct influence on the basic phenomena occurring in crystallization is the supersaturation, often defined in terms of solute concentration.

Feedback control strategies in which the jacket temperature is computed based on on-line measurements of the solute concentration in order to follow a given supersaturation profile have been widely investigated (see e.g. [4] and [5]). In literature, they are known as C-control strategies [3]. In general, C-control was shown to give better performance compared to T-control, particularly in terms of reproducibility of the final product. A condition for the implementation of C-control is obviously that accurate on-line concentration measurements are available.

At laboratory scale, the use of technologies such as ATR-FTIR spectroscopy for measurements of concentration has already been proven (see e.g. [6]), and C-control has been succesfully implemented. However, at full industrial scale, the robustness and precision of such measurements requires further investigation. In those cases, accurate concentration measurements can only be obtained from laboratory analysis of samples collected throughout the batch and are only available at the end of a batch. This makes on-line C-control not yet feasible in an industrial environment.

In such a situation where concentration measurements are only available off-line, we can nevertheless achieve supersaturation tracking by using the information batchwise. Iterative Learning Control (ILC) is known to be an effective way to improve the tracking performance of uncertain dynamical systems that operate repetitively [7]. In ILC, measurements are collected after each iteration (in our case after each batch) to improve the tracking performance at the next iteration (in our case the tracking of a supersaturation profile).

A well-known drawback of ILC is nevertheless the inability to cope efficiently with unknown disturbances that are different from iteration to iteration. Consequently, an ILC approach alone might not be sufficient to control supersaturation in the crystallizer in presence of system disturbances.

In this paper, we propose a novel control strategy to track efficiently a supersaturation profile under the presence of unknown disturbances and process uncertainties. This strategy, inspired by the master-slave configuration, exploits the fact that concentration measurements are only available offline, but temperature measurements are readily available online. In fact, our strategy combines a slave temperature feedback controller and a master ILC algorithm.

Based on the desired supersaturation profile and the off-line concentration measurements from the previous batches,

The authors are with the Delft Center for Systems and Control, Delft University of Technology, Mekelweg 2, 2628 CD Delft, The Netherlands.
m.forgione@tudelft.nl
ali.mesbah@tudelft.nl
x.j.a.bombois@tudelft.nl
p.m.j.vandenhof@tudelft.nl

the ILC algorithm computes after each batch an improved profile T^r for the temperature in the crystallizer. This profile is then used in the next batch as a new reference for the (slave) feedback loop. The controller in this feedback loop is designed to reject the system disturbances as efficiently and as fast as possible to decrease their influence on the supersaturation control. This improves the tracking efficiency of the ILC algorithm.

The ILC algorithm used in this paper is based on the so-called two-step procedure [8]. After each batch, the available model of the dynamics between the temperature reference T^r and the supersaturation is adapted in a non-parametric way based on the measurements collected during the previous batch. The next temperature reference is then obtained by minimizing a quadratic criterion involving the tracking error for the supersaturation as well as a regularization term in order to avoid large modifications of T^r from batch to batch. Such an approach is called *Quadratically Optimal Design* or Q-ILC [9].

The ILC algorithm presented in this paper is based on a nonlinear first-principles nonlinear model of crystallization. In the literature, another applications of ILC for supersaturation control was presented in [10]. In comparison with the latter contribution, the advantage of our approach is twofold. First, the master-slave configuration which is an asset in the presence of disturbances. Second, the use of the first-principles model in the algorithm as opposed to a linearized model used in [10], which is a good approximation of the dynamics only along the time-varying working point.

II. MODEL OF BATCH COOLING CRYSTALLIZATION

Under the assumptions of well-mixed suspension, no breackage and agglomeration, and nucleation occurring at negligible size only, the dynamics of a batch crystallization process are described by the *Population Balance Equation* (PBE) [11]:

$$\frac{\partial n(L,t)}{\partial t} = -\frac{\partial \big(Gn(L,t)\big)}{\partial L}$$
$$n(0,t) = \frac{B}{G} \tag{1}$$

where $n(L,t)$ is the *Crystal Size Distribution* (CSD), representing the number density of crystals with length L at time t, divided by the total volume of the crystallizer V. B and G are terms representing the birth of new crystals (nucleation) and the growth of existing crystal respectively. B and G are, in general, functions of the temperature T, the CSD and the supersaturation S. This last quantity is the difference between the actual solute concentration in the liquid phase C, and the equilibrium concentration given by the solubility $C_s(T)$:

$$S = C - C_s(T). \tag{2}$$

At this point let us define for convenience the i-th moment of the CSD as

$$m_i(t) \triangleq \int_0^\infty L^i n(L,t)\, dL. \tag{3}$$

The concentration C is a static function of the third moment m_3, due to the crystal mass balance:

$$C = C_0 - 10^{-3}\rho_c k_v(m_3(t) - m_3(0)) \tag{4}$$

where C_0 is the initial concentration, ρ_c is the crystal density and k_v is the shape factor of the crystals. The solubility line $C_s(T)$ can be approximated as a low-order polynomial in T:

$$C_s(T) = a_0 + a_1 T + a_2 T^2 + a_3 T^3. \tag{5}$$

Several models for B and G have been proposed in literature: a common choice for control applications, which gives a reasonable fit to experimental data, is given by [11]:

$$B = k_b m_3 S^b \qquad\qquad G = k_g S^g \tag{6}$$

where k_b, k_g, b, g are kinetic parameters.

Adopting this model, the time evolution of the moments of the CSD can be exactly expressed by a set of differential equations known as the moment equations [12]:

$$\begin{aligned} \frac{dm_0}{dt} &= B \\ \frac{dm_i}{dt} &= iGm_{i-1} \qquad i = 1,2,3. \end{aligned} \tag{7}$$

The temperature dynamics, ignoring the heat of crystallization, are described as

$$\frac{dT}{dt} = \frac{UA(T_J - T)}{\rho c_p V} \tag{8}$$

where U is the heat-transfer coefficient, A is the heat-transfer area, ρ is the density of the slurry and c_p is the heat capacity of the slurry. T_J, the jacket temperature, is considered as the input variable of the system. Dynamic equations (7) and (8), together with kinetic expressions (6), the mass balance (4), the expression of the solubility line (5) and the definition (2) of supersaturation form, together with a given initial condition, a solvable set of Differential Algebraic Equations (DAEs). These DAEs can be transformed to Ordinary Differential Equations (ODEs) via direct substitution. The parameters of the model are reported in the Appendix I.

In our simulation environment, the outputs of the system are the reactor temperature $T(t)$ and the solute concentration $C(t)$. They are collected at a sampling rate $t_s = 5s$.

A. Disturbances and model uncertainty

Measurements $\tilde{C}(t)$ and $\tilde{T}(t)$ of $C(t)$ and $T(t)$ are assumed to be corrupted by additive measurement noise e_C and e_T respectively. e_C and e_T are modeled as realizations of independent white gaussian variables with standard deviation 0.1 ºC and 0.4 g/L respectively.

The jacket temperature T_J is perturbed by a low-frequency disturbance modeled as an autoregressive stochastic process of order 1 with standard deviation $\sigma_{AR} = 0.25$ ºC :

$$\delta_T(t+1) = a\delta_T(t) + e(t) \tag{9}$$

where $a = 0.9895$ and $e(t)$ is white gaussian noise with variance $\sigma_e^2 = \sigma_{AR}^2(1-a^2)$. The noise realizations e_C, e_T, δ_T are different for each batch since the disturbances are assumed to have a non-reproducible nature.

The dynamics of the process are assumed to be exactly described by the equations previously introduced. However, the kinetic parameters $\theta = \begin{bmatrix} k_b & b & k_g & g \end{bmatrix}^\top$ in (6) are not usually known accurately. In this work, we will assume that the actual value θ_0 lies in a given box region Θ centered around a nominal $\hat{\theta}$. The width of the region is $\pm 10\%$ of the nominal values of each parameter:

$$0.9\hat{\theta}_i \leq \theta_{0,i} \leq 1.1\hat{\theta}_i \qquad i = 1 \ldots 4. \tag{10}$$

The other parameters of the model are assumed to be known exactly.

B. Discrete finite-time representation

Consider the system in a finite-time span and with a fixed-step integration scheme, for a given initial condition. Define N as the number of samples corresponding to a batch. Then, the output vector $\mathbf{S} \in \mathbb{R}^N$ containing the supersaturation at the sampling time is a nonlinear static function of the input vector $\mathbf{T_J} \in \mathbb{R}^N$ of the jacket temperature. This function depends on the parameters θ:

$$\mathbf{S} = F_{ST_J}(\mathbf{T_J}; \theta). \tag{11}$$

A Runge-Kutta scheme with sampling time $t_d = 5$s is used for discretization of the continous time equations of the model (note that we choose $t_d = t_s$ for simplicity).

In the following, we shall adopt the bold-face notation for vectors in $\mathbb{R}^N$, while $F_{YU}(\cdot)$ has to be interpreted as the function from the input vector $\mathbf{U}$ to the output vector $\mathbf{Y}$.

III. ITERATIVE LEARNING CONTROL FOR BATCH CRYSTALLIZATION

We devise in this section an ILC scheme for supersaturation control of the cooling crystallization system described in the previous section. Taking a look at the model equations, the jacket temperature T_J may be considered as the input, and therefore we could design an ILC scheme based on T_J directly.

However, due to the presence of disturbances on the temperature dynamics, we prefer to design a PI temperature controller for the crystallizer temperature T and to use the set point of the controller T^r as input for the ILC algorithm.

The overall ILC+PI control scheme is sketched in Figure 1. The two rightmost blocks represent the batch crystallizer, whose dynamics is conceptually split into two parts: the temperature dynamics corresponding to equation (8) and the crystallization dynamics corresponding to equation (7). The two leftmost blocks represent the control system: the PI temperature controller and the ILC controller, which drives the reference of the latter. The signals coming and departing from the ILC block are updated off-line only (i.e. from one batch to the other), and are indicated by dashed lines. All other signals are represented by continuous lines because their value is updated during the same batch, at sampling time t_s.

The temperature controller design is based on the temperature dynamics (8) and the specifications of the disturbances e_T and δ_T.
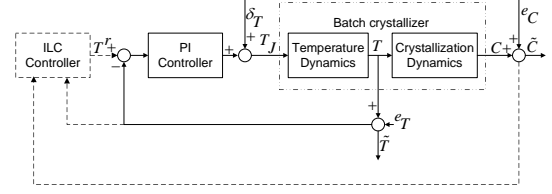

Fig. 1. The overall ILC+PI control scheme

Given the first order dynamics, a PI controller is considered to be sufficient. This PI controller is determined by the transfer function

$$C(s) = K_P + \frac{K_I}{s} \tag{12}$$

where K_P and K_I are set to

$$K_P = \frac{\rho c_p V}{t_{cl} U A} \qquad K_I = \frac{1}{t_{cl}}. \tag{13}$$

t_{cl} is a free parameter which is the time constant of the closed-loop system. A small time constant is beneficial for the rejection of the noise δ_T, while it is detrimental to the rejection of e_T. An appropriate choice is thus the result of a trade-off between different objectives; in our case, $t_{cl} = 2$ min was found to give a good result.

A discrete time version of this PI controller with sampling time t_s is implemented in the simulation model.

In order to test the robustness of the proposed scheme, the model used by the ILC algorithm is based on the response from T to S with nominal value $\hat{\theta}$ for the kinetic parameters

$$\hat{\mathbf{S}} = F_{ST}(\mathbf{T}^r; \hat{\theta}) = \hat{S}(\mathbf{T}^r) \tag{14}$$

while the true dynamics of the system are governed by

$$\mathbf{S} = F_{ST^r}(\mathbf{T}^r; \theta_0) = S(\mathbf{T}^r). \tag{15}$$

We consider the problem of following a desired supersaturation trajectory $\bar{\mathbf{S}}$ as closely as possible in N_{it} iterations (batches).

To design the nonlinear iterative learning controller, we employ the strategy discussed in [8]. At each iteration k of the algorithm, the following steps are executed:

1) The temperature profile $\mathbf{T}_k^r$ is set as the input to the temperature controller of the true system and the noisy measurements $\tilde{\mathbf{C}}_k, \tilde{\mathbf{T}}_k$ are collected.
2) Low-pass filtering is applied to the measurements and supersaturation $\tilde{\mathbf{S}}_k$ is computed via Equation (2).
3) A correction vector is computed as

$$\boldsymbol{\alpha}_{k+1} = \arg\min_{\alpha \in \mathbb{R}^N} \|\tilde{\mathbf{S}}_k - (\hat{S}(\mathbf{T}_k^r) + \boldsymbol{\alpha})\|^2 + S_\alpha \|\boldsymbol{\alpha} - \boldsymbol{\alpha}_k\|^2 \tag{16}$$

where S_α is the iteration-dependent scalar:

$$S_\alpha = \begin{cases} 0, & k = 0 \\ 1, & k \in [1 \ldots 4] \\ 5, & k \geq 5 \end{cases} \tag{17}$$

and a corrected model

$$S^c_{k+1}(\mathbf{T}^r) = \hat{S}(\mathbf{T}^r) + \boldsymbol{\alpha}_{k+1} \tag{18}$$

is found.

4) The corrected model is used to compute the temperature profile for the next iteration

$$\mathbf{T}^r_{k+1} = \arg \min_{\mathbf{T}^r \in \mathbb{R}^N} \|\overline{\mathbf{S}} - \mathbf{S}^c_{k+1}(\mathbf{T}^r)\|^2 + \lambda \|\mathbf{T}^r_{k+1} - \mathbf{T}_k\|^2 \tag{19}$$

where λ is the iteration-dependent scalar:

$$\lambda = \begin{cases} 0, & k \in [0 \dots 10] \\ 1, & k \in [11 \dots 20] \end{cases} \tag{20}$$

The initial temperature profile is found as the solution of the following min-max optimization problem

$$\mathbf{T}^r_1 = \arg \min_{\mathbf{T} \in \mathbb{R}^N} \max_{\theta \in \Theta} \|F_{ST}(\mathbf{T}, \theta) - \overline{S}\|^2 \tag{21}$$

where Θ is the uncertainty region defined in (10).

S_α and λ are free tuning parameters of the algorithm; the choice implemented in this paper was found to give a good trade-off between rapid convergence and noise attenuation.

Optimization problems (19) and (21) are solved numerically using the active-set algorithm of the Matlab function `fmincon`. Model equations are integrated at each step of the optimization in order to evaluate the objective function. The gradient of the objective function with respect to the input is obtained via finite differences. In order to reduce the dimensionality of the problem, $\mathbf{T}^r$ is sub-parametrized as the integral of a piecewise linear signal passing through $n_p = 40$ equally spaced time instants. This kind of optimization strategy is known as *single shooting* in literature, and was applied to similar problems in [13].

In general, there is not a definitive guarantee that the numerical solution of such Nonlinear Optimization Problems (NLPs) would converge to a global optimum since the optimization algorithm may be trapped in different local optima depending on the initial guess. A similar event would have a negative influence on the performance of the ILC scheme. However, in the case presented in this paper this situation does not seem to occur. The influence of the initial guess on the optimization result is always very small and most likely caused by the numerical tolerance on the termination condition of the optimizer. A minor impact on the performance of the ILC scheme is however given by the sub-parametrization of the input, as discussed in the next section.

IV. SIMULATION RESULTS

In this section, we evaluate the performance of the ILC algorithm described in the previous section on four different test cases. For all cases, $N_{\text{it}} = 20$ iterations of the algorithm are executed. In a real setup, each iteration of the algorithm corresponds to the execution of a batch of duration $t_f = 180$ min. The tracking problem is always the same: to attain a constant supersaturation level $\overline{\mathbf{S}}(t) = 2.5$ g/L throughout the batch, starting from the temperature $T_0 = 38\ ^oC$ and concentration $C_0 = C_s(T_0) + 2.5$ g/L at time $t_0 = 0$.
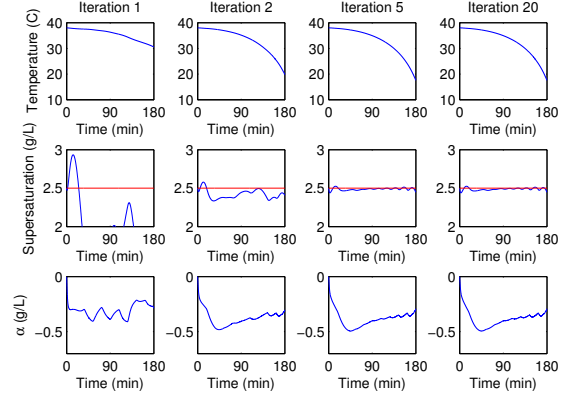

Fig. 2. Case 1: iterations 1,2,5,20

The true parameter θ_0 is kept the same for all cases; however, the algorithm has no information about θ_0 as it is designed based on the nominal value $\hat{\theta}$.

Case 1

In this simulation, disturbances e_C, e_T and δ_T are set to 0. Temperature, supersaturation and the vector $\boldsymbol{\alpha}$ for iterations 1, 2, 5 and 20 are shown in Figure 2. The algorithm converges in a few iterations close to the set-point despite the model-plant mismatch. Convergence is essentially achieved at the third batch and the solution is stable in the following iterations. Also the vector $\boldsymbol{\alpha}$ converges to a fixed value.

Case 2

In this simulation, the presence of the disturbances e_C, e_T and δ_T is taken into account. Results for the simulation are shown in Figure 3. The performance of the algorithm remains very good and the effect of disturbances is attenuated as expected by the PI controller. Note that the effect of such disturbances on the output S is larger at the beginning of the batch (high temperature) and decreases towards the end (low temperature). Indeed, the sensitivity of the output S to temperature fluctuations is larger at high temperature due to the higher steepness of the solubility line (5).

Note also that the vector $\boldsymbol{\alpha}$ is much smoothened from iteration 5 to 20 owing to the S_α term in (16) and still shows a similar shape as in Case 1.

Case 3

In this simulation, the presence of structural model-plant mismatches is considered. The process is assumed to generate a significant amount of heat, sufficient to influence the temperature dynamics. This can be modeled by modifying equation (8) to

$$\frac{dT}{dt} = \frac{UA(T_J - T)}{\rho c_p V} - \frac{3\rho_c k_v \Delta H G m_2}{\rho c_p} \tag{22}$$

where ΔH is the crystallization heat. Furthermore, a different model of the nucleation dynamics is assumed for the real system, i.e. the birth rate B is modified to

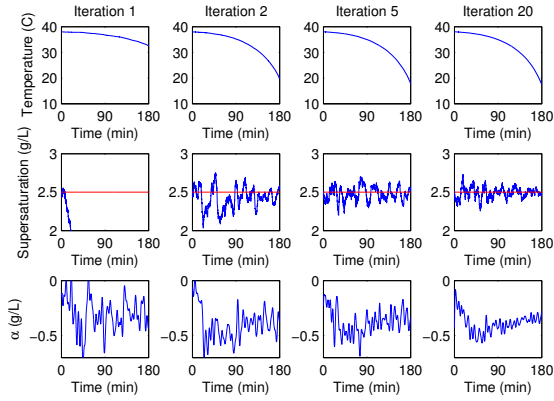$$B = k_b m_2 S^g. \tag{23}$$

Fig. 3.   Case 2: iterations 1,2,5,20
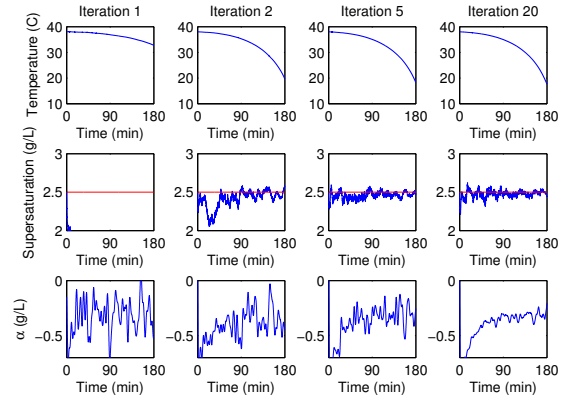

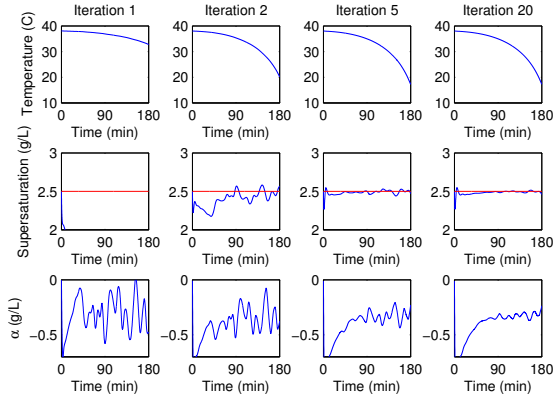Fig. 5.   Case 4: iterations 1,2,5,20

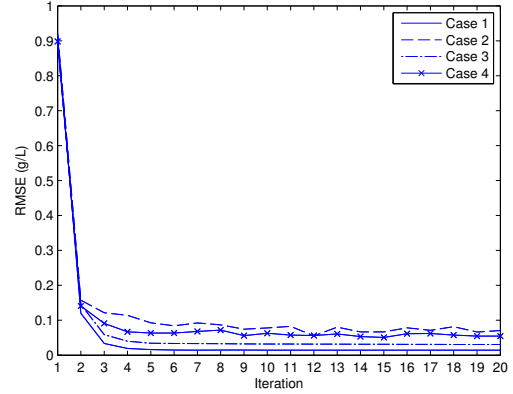
Fig. 4.   Case 3: iterations 1,2,5,20

Fig. 6.   RMSE of the tracking error vs. iteration number

However, no information about this difference in behavior is used by the algorithm. The results of this simulation are reported in Figure 4. The algorithm can cope with this kind of structural uncertainty very well; almost the same tracking performance as in Case 1 is achieved. Note that the vector $\boldsymbol{\alpha}$ converges to a value that is different from Case 1. This is reasonable, as a different model correction is required in this case to cope with the different mismatch.

Case 4

In this simulation, the structural mismatch as in Case 3 and the disturbances as in Case 2 are considered altogether. The results of this simulation are shown in Figure 5. Again, the achieved tracking result is satisfactory. The vector $\boldsymbol{\alpha}$ also converges to a similar value as in Case 3 as expected.

Overall Results

The *Root Mean Square Error* (RMSE) of the supersaturation tracking error is plotted against the iteration number for all cases in Figure 6. In all cases, a good tracking result is mostly achieved already at the third iteration and the RMSE of the tracking error at iteration 20 is less than 0.1 g/L. In Cases 1 and 3 the RMSE seems to converge to a very small value that is however not exactly 0, even though perfect tracking would be in principle possible. This small residual error is the combined effect of the input sub-parametrization used for the solution of (19) and of the inexact model correction performed in ILC. In Cases 2 and 4 the RMSE seems to converge to a slightly higher value, mainly due to the effect of the disturbances. For Case 2, simulations with 100 different realization of the parameter vector θ_0 were performed. The RMSE at the iteration 20 has an average of 0.08 and standard deviation 0.02 g/L.

For sake of comparison with pure open loop control, the PI controller was removed and the optimal solution was implemented direcly on T_J. Even under the assumption of perfect knowledge of the dynamics, the RMSE is about 0.4 g/L in this case due to the effect of the disturbance δ_T.

V. CONCLUSION

We have presented an ILC strategy for supersaturation control in batch cooling crystallization. Coupled with a PI temperature controller, the proposed scheme shows good convergence properties and robustness with respect to disturbances and model uncertainties. The performance level evaluated in terms of RMSE of the supersaturation tracking error is very good in all the cases analyzed. Most likely, such a control scheme is appropriate for many industrial crystallization processes.

The ILC strategy much resembles an Iterative Identification Control (IIC) approach in which at each iteration

Name	Description	Value	Units
ρ_c	Crystal density	1130	Kg/m^3
k_v	Crystal shape factor	1	-
T_0	Initial temperature	38	^{o}C
ρ	Slurry density	789	Kg/m^3
c_p	Slurry heat capacity	4185	J /(^{o}C Kg)
V	Crystallyzer volume	0.905	m^3
UA	Product heat-transfer area	$1.49 \cdot 10^5$	J /(min ^{o}C)
a_0	Coefficient 0 solubility	$27.8428 \cdot 10^{-3}$	Kg/L
a_1	Coefficient 1 solubility	$2.0891 \cdot 10^{-3}$	Kg/(L ^{o}C)
a_2	Coefficient 2 solubility	$-0.0311 \cdot 10^{-3}$	Kg/(L ^{o}C^2)
a_3	Coefficient 3 solubility	$0.0017 \cdot 10^{-3}$	Kg/(L ^{o}C^3)
ΔH	Crystallization heat	$-3000 \cdot 10^3$	J/Kg
k_b	Nucleation parameter	$1.057 \cdot 10^{13}$	1/(m^3 min)
b	Nucleation exponent	1.7	-
k_g	Growth parameter	$5.0 \cdot 10^{-4}$	m /min
g	Growth exponent	1.1	-

TABLE I

PARAMETERS OF THE MODEL

1) we perform a parameter identification step, eventually propagating the information of the previous batches as an *a priori* term in a Bayesian framework;
2) we compute the optimal input based on the new model and implement it in the real system.

The main differences in the ILC strategy are:

- we do not make direct use of statistical hypotheses (while we formulate IIC in a stochastic setting);
- we consider the model update to be valid in a neighborhood of the current trajectory only.
- we update a set of additional parameters $\boldsymbol{\alpha}$, instead of the physical model parameters.

The update used in ILC is likely to cope with under-modelling better than IIC due to the flexibility given by the vector $\boldsymbol{\alpha}$. However, noise handling and tuning of the learning weights il not straightforward in the ILC case.

In the future, the ILC algorithm could be introduced in a stochastic setting in order to make the tuning procedure more rigorous.

APPENDIX I
MODEL DETAILS

A. Parameters

Model parameters are reported in Table I. For the uncertain parameters, the nominal value $\hat{\theta}$ is presented.

B. Initialization

An initial distribution, leading to initial values of the moments, has to be given in order to start the simulations.

In this work we assume that the CSD at time 0 $n_0(L)$ has the shape of the positive part of a parabola centered at the mean size $L_0 = 40 \ \mu m$ and having width $v_s = 20 \ \mu m$:

$$n_0(L) = \max\left(0, a(L - (L_0 + v_s))(L - (L_0 - v_s))\right). \quad (24)$$

The constant a is found such that the total mass of crystal in the initial distribution is equal to $M_s = 1$Kg:

$$M_s = \rho_c k_v V \int_0^\infty L^3 n_0(L) \, dL. \quad (25)$$

The initial moments are obtained according to (3):

$$m_i(0) = [1.328 \times 10^{11}, \ 5.314 \times 10^6, \ 223.2, \ 0.0098] \quad (26)$$

C. Rescaling

For numerical reason, the model is modified by rescaling crystal number by a factor s_N and crystal length by a factor s_L in the software implementation.

In the new variables, the rescaled CSD $n'(L', t)$ is expressed in $(\# \cdot s_N/(m^3 \cdot s_L m)$ with $s_N = 10^{-10}$ and $s_L = 10^4$. The original moments m_i are in 1:1 correspondence with the rescaled moments m_i' according to the formula

$$m_i' = s_N s_L^i m_i \quad (27)$$

System equations can be adapted in the rescaled variables by modifying the kinetic parameters:

$$k_g' = s_L k_g \qquad k_b' = \frac{k_b}{s_L^3} \quad (28)$$

and mass balances involving m_3, according to (27). The initial state has also to be adapted, again according to (27).

Adopting this transformation, all the model states are kept in the same numerical range (approximately 0 to 100). This is particularly useful when the model is used for optimization.

REFERENCES

[1] A. Myerson, *Handbook of industrial crystallization*. Butterworth-Heinemann, 2002.
[2] A. Mesbah, "Optimal operation of industrial batch crystallizers," Ph.D. dissertation, Delft University of Technology, 2010.
[3] M. Fujiwara, Z. Nagy, J. Chew, and R. Braatz, "First-principles and direct design approaches for the control of pharmaceutical crystallization," *Journal of Process Control*, vol. 15, no. 5, pp. 493–504, 2005.
[4] W. Xie, S. Rohani, and A. Phoenix, "Extended kalman filter based nonlinear geometric control of a seeded batch cooling crystallizer," *The Canadian Journal of Chemical Engineering*, vol. 80, no. 1, pp. 167–172, 2002.
[5] Z. Nagy, J. Chew, M. Fujiwara, and R. Braatz, "Comparative performance of concentration and temperature controlled batch crystallizations," *Journal of Process Control*, vol. 18, no. 3-4, pp. 399–407, 2008.
[6] T. Togkalidou, M. Fujiwara, S. Patel, and R. Braatz, "Solute concentration prediction using chemometrics and atr-ftir spectroscopy," *Journal of Crystal Growth*, vol. 231, no. 4, pp. 534–543, 2001.
[7] H. Ahn, Y. Chen, and K. Moore, "Iterative learning control: Brief survey and categorization," *Systems, Man, and Cybernetics, Part C: Applications and Reviews, IEEE Transactions on*, vol. 37, no. 6, pp. 1099–1121, 2007.
[8] M. Volckaert, M. Diehl, and M. Swevers, "A two step optimization based iterative learning control algorithm," in *Dynamic Systems and Control Conference*, Cambridge, Massachusetts, USA, September 2010, pp. 579–581.
[9] D. Bristow, M. Tharayil, and A. Alleyne, "A survey of iterative learning control," *Control Systems Magazine, IEEE*, vol. 26, no. 3, pp. 96–114, 2006.
[10] J. Zhang, J. Nguyan, Z. Xiong, and J. Morris, "Iterative learnig control of a crystallization process using batch wise updated linearized models," in *Computer Aided Chemical Engineering*, 2009, pp. 387–392.
[11] A. Randolph and M. Larson, *Theory of particulate processes*. Academic Press San Diego, CA, 1971.
[12] H. Hulburt and S. Katz, "Some problems in particle technology:: A statistical mechanical formulation," *Chemical Engineering Science*, vol. 19, no. 8, pp. 555–574, 1964.
[13] A. Mesbah, A. Huesman, H. Kramer, Z. Nagy, and P. Van den Hof, "Real-time control of a semi-industrial fed-batch evaporative crystallizer using different direct optimization strategies," *AIChE Journal*, vol. 57, no. 6, pp. 1557–1569, 2011.